FINE- AND SUPERFINE-STRUCTURE EFFECTS IN NUCLEAR EXCITATIONS AND NEUTRON RESONANCES

S. I. Sukhoruchkin, Z. N. Soroko, D. S. Sukhoruchkin

Petersburg Nuclear Physics Institute, Gatchina, Russia

Abstract

As a continuation of the previous publication NRF-3 in LB I/24, Springer and compilation of low-lying levels in LB 1/19 we started collection of recently produced nuclear data important for the check of fine- and superfine-structures in neutron resonance spacing and positions. These structures are considered as a part of a common tuning effect in nuclear excitations and nuclear binding energies. Tuning effect consists in an appearance of stable mass/energy intervals close (or rational) to the electromagnetic mass differences of the nucleon, electron and pion and the presence of the scaling effects similar to the QED radiative correction for the electron. We observe long-range correlations in all sets of data (excitations E^*, neutron resonances and binding energies E_B).

1 Introduction

In previous works [1,2] motivation for production of neutron resonance parameters compilation NRF-3 [3] was described. There is a great advantage of new data over existed in the published papers due to continuation of data-production by GELINA and other spectrometers. GELINA has a superior energy resolution in measurements at its long base-lines. There is a hope that new results will be obtained not only in CERN n-Tof measurements but also at GELINA. Recent plans for measurements with RPI and ORELA accelerators and with DANCE were considered in [3]. As an example, in Table 1 numbers of resonances (N_B) measured by Schillebeeackx (GELINA), Fujii (n-Tof) and Koehler (ORELA) not included in [3] are presented together with the total number of resonances in NRF-3.

Table 1. Numbers of neutron resonances in new measurements (N_B) and NRF-3 (N).

Isotope	N_B/N	Isotope	N_B/N	Isotope	N_B/N	Isotope	N_B/N
^{103}Rh	many/294	^{187}Os	300/311	^{194}Pt	337/8	^{196}Pt	231/6
^{186}Os	120/133	^{188}Os	110/115	^{195}Pt	388/45	^{206}Pb	many/772

Results obtained in the previous study of nonstatistical effects in neutron resonances described in [4-14] are presented in Table 2 where the tuning effects in particle masses (three first sections in the Table) and in nuclear excitations and neutron resonances (two bottom sections) are given together. The first section contains top-quark mass m_t, vector boson mass M_Z and preliminary values (M^{L3}, M_H) of mass-groupings observed at LEP. Relation 3:2:1 in their values is discussed in [4-10] (M_H – Higgs-boson mass). Tuning effect in particle masses is represented by muon and pion masses and nucleon Δ-excitation which are close to integers with a common period δ=16m_e (numbers n=13,17,18 in the top line of Table 1).

Values of particle masses and stable nuclear intervals are presented as the parameter δ=16m_e multiplied by the factor $\alpha/2\pi$ of the power x (x=-1,0,1.2). This QED parameter $\alpha = 137^{-1}$ is used to compare values situated one under another in different sections of the Table. M_H and the main QCD low-energy parameter m_π are boxed.
The third section of the top part of the Table contains accurately known value m_e, mass splitting of the nucleon (δm_N) and the shift of accurately known neutron mass relative to integer numbers N=115×16-1 of the m_e (boxed). Ratio δ_N/161.6(1) keV=8.002(2) and similar observed [16-19] long-range correlations in nuclear binding energies demonstrate the fact that nucleon masses and nucleon interactions described by QCD – theory of strong interaction – show tuning effects which could be observed also in nuclear excitations (E^*) and nuclear binding energies (E_B). It was discussed long ago that there is some sort of a correspondence between E^* and E_B which is responsible for empirically observed correlations in neutron resonance positions (differences between E^* and S_n=ΔE_B).

Table 2. Presentation of parameters of tuning effects in particle masses (three upper parts with x=-1,0,1,2) and in nuclear excitations by the expression (n×16$m_e(\alpha/2\pi)^x$) × m with QED parameter $\alpha = 137^{-1}$. One asterisk marks stable nuclear intervals observed earlier in excitations and neutron resonances [5-8], two asterisks mark intervals found in this work; ε_{np} is the parameter of nucleon residual interaction [20]; values related to (2/3)m_t=M_H with the QED parameter α_Z=129^{-1} and the shift in the neutron mass are boxed.

x	m	n=1	n=13	n=14	n=16	n=17	n=18
-1	3/2				m_t=171.2		
GeV	1/2				M^{L3}=58		
	1		M_Z=91.2		$\boxed{M_H=115}$		
0	1	16m_e=δ	m_μ=105.7		(f_π=131)	$\boxed{m_\pi - m_e}$	m_Δ-m_N/2=147
MeV	3				M''_q=m_ρ/2	M'_q=420	M_q=441=ΔE_B
1	1					$\boxed{\text{n}\delta\text{-}m_n\text{-}m_e=161.6(1)}$	$\boxed{170=m_e/3}$
keV	3						m_e=510.99891
	8					δm_N=1293.34(1)	
1	1	9.5=δ'	123	132	152	160-162*	170=ε_o/6,168*
keV	2	19	247**	264*	303	321*	341*, ε_{np}
	2		245**			322**	340**
	3		369**	397	455	482**,481*	511*=ε_o/2
	3		367*			486*	511**
	4	39	492*	532*	606**	647*,644*	681-685*
	4		490**	530*		648**,646*	683**
	5		611**				
	5		611**				
	6		736**		910*	965*	1020**,1024**
	6		739*			964*	1022*
	8		984*	1060**	1212*	1293*=D_o	1360-1364*
	8		983**	1061*		1293**	1366*
	12		1475*				
2	1	11=δ''	143		176	187	D in neutron
eV	4,8	44	570*			749-1500*	resonances

2 Tuning effects in nuclear excitations

The grouping of excitation energies can be explained by theoretical models. For example, maximum at E^*=1212 keV in E^*-distribution for all nondeformed nuclei (A$\leq$150) shown in Fig.1 (top left) corresponds to stable values of 2^* excitations in Z-magic tin isotopes.

Table 3. Energy levels of Z=33-35 nuclei with E^* (keV) close to ε_o=1022 keV=$2m_e$ [21].

^AZ	^{74}As	^{76}As	^{73}Se	^{75}Se	^{77}Se	^{80}Br	^{80}Br	diff.	^{81}Br	^{82}Br	^{83}Br
$E^*(\approx \varepsilon_o)$	1021.5	1023.2	1021.9	1020.5	1024.1	1021.3	1022.4	1.1	1023.7	1022.5	1021.5

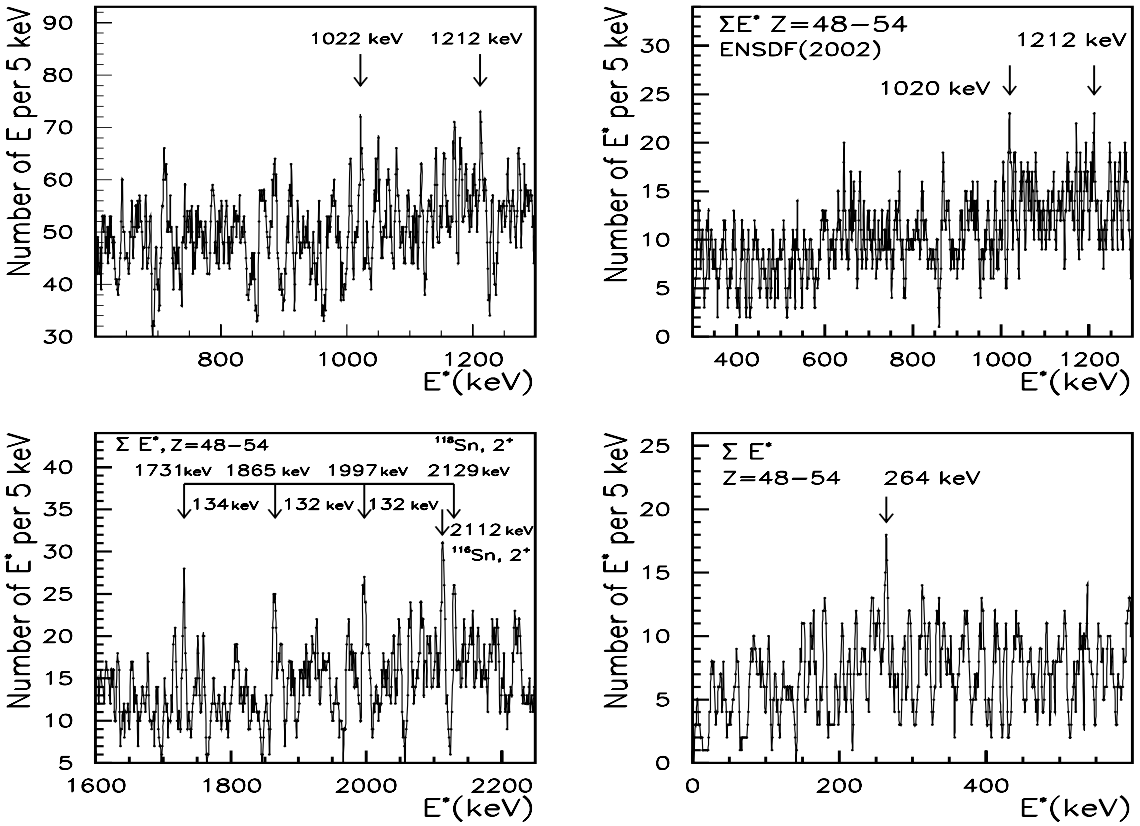

Fig.1. *Top:* Total distribution of excitation energies E^* of all nuclei with A$\leq$150 [21] (*left*); The same for nuclei with Z=48-52 in three different energy regions (*top right and bottom*).

Another maximum in this distribution at $E^*=\varepsilon_o$=1022 keV corresponds to effects in several groups of nuclei, for example, with Z=33-35 (Table 3). Here the grouping at $E^*=\varepsilon_o$ is accompanied by a small splitting in ^{82}Br (about 1.1 keV or $\varepsilon_o \times 10^{-3}$). Presence of small splitting in odd-odd spherical nuclei was discussed in [12,21] during the analysis of energies of γ-ray transitions performed in [22]. The nonstatistical character of spacing D in 8 nuclei was represented by the expression $E_\gamma=D=(\varepsilon_o$=1021 keV)/N (N-integer, see also [21,22]). The first time such effect was mentioned in [23].

The stable character of excitations of E^*=1020 keV in nuclei around tin (Fig 1 top right [21]) is supported by stable spacing $D=\varepsilon_o$ in ^{115}Sn [19]. In nuclei around tin maxima in E^*-distribution (Fig.1 bottom left) correspond to stable 2^+ excitations E^*=2112 keV and 2129 keV in ^{116,118}Sn. We observe a series of maxima separated by the interval 133 keV=2129 keV/16 and stable E^*=264 keV=2119 keV/8 (Fig.1 bottom right).

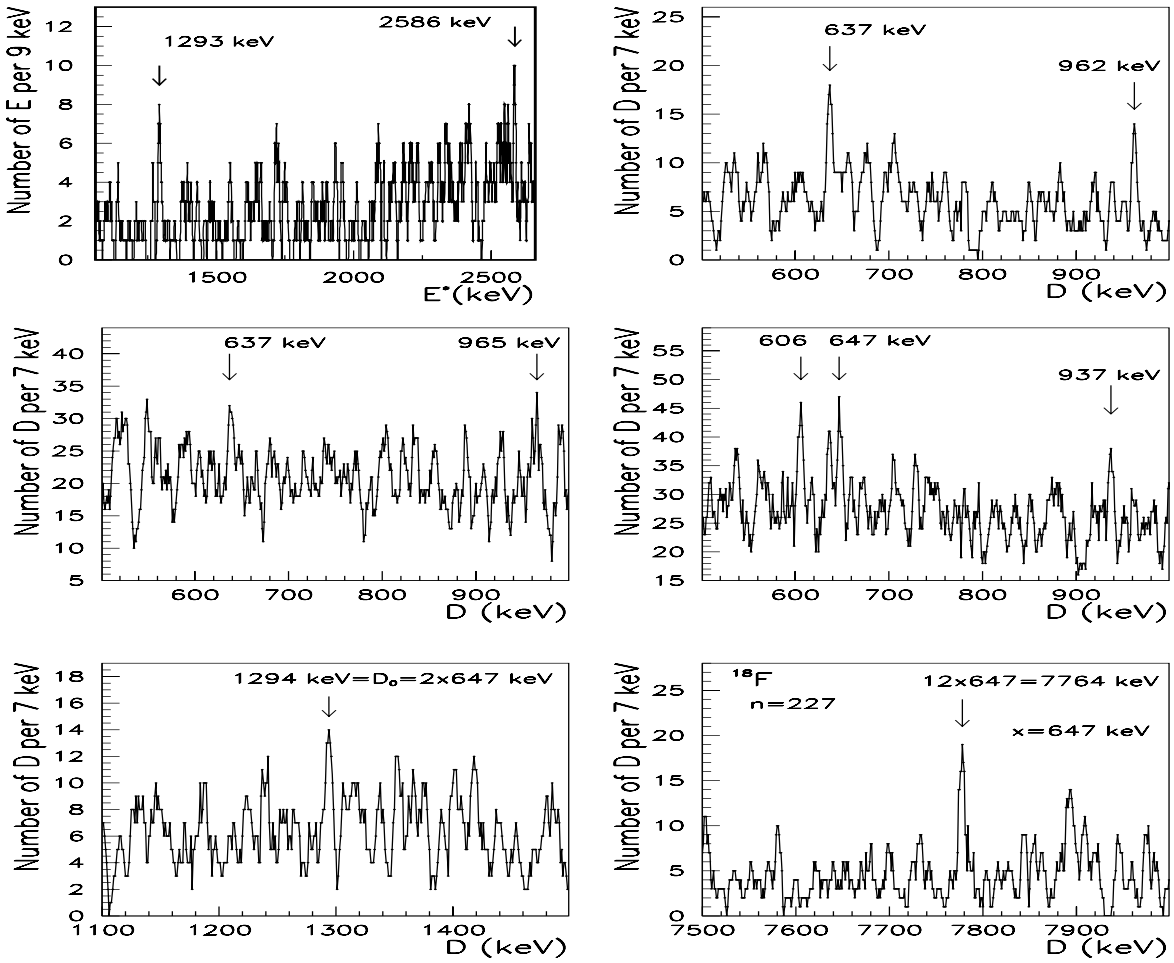

Fig.2. *Top:* Total distribution of excitation energies E^* in Z-odd nuclei with Z$\leq$29 [19] (*left*); Spacing distributions of low-lying levels in ^{18}F and ^{22}Na (*top right, center left*, n=76 and 145). Spacing distribution of all known levels of ^{18}F (number of levels n=227 [24,25]) (*center right*); *Bottom:* Distribution of intervals adjacent to x=$D_o/2$ in ^{18}F (maxima at D^{AIM}=D_o and $6D_o$).

The grouping of excitations in light nuclei (Z$\leq$29) at values E^*=D_o coinciding with nucleon mass splitting δm_N=1293.3 keV and $2D_o$ (Fig.2 top left) was noticed in [19,21].

The following confirmation of these intervals was obtained. Clear nonstatistical effect was found in D-distributions of ^{18}F and ^{22}Na (nuclei differing by α-cluster) shown in Fig.2. Stable intervals D=637 keV are exactly equal to the half of the first 2^+ excitation E^*=1274.5 keV in ^{22}Ne (another common interval D=962-965 keV is close to $(3/4)D_o$=970 keV [17]). The inclusion in the analysis of all known excited states of ^{18}F, mainly from charged-particles resonances data (n=227 [25]) resulted in the distribution shown in Fig.2 (center right) where the interval 647 keV=$D_o/2$ equal to a half of the first 2^+ excitation D=1294.8 keV between T=1 levels of ^{24}Na (657 keV-1952 keV) is more pronounced than D=637 keV in low-energy data. To check this interval we use so-called AIM-method (Adjacent Interval Method) which consists of fixation of all levels separated by intervals (x) forming maximum in D-distribution (here, interval to D=x=647 keV) and calculating distribution of all spacing (D^{AIM}) from fixed levels to all other levels in the spectrum. Obtained maxima at D^{AIM}=1294 keV=D_o=2$\times$647 keV and 12$\times$647 keV=$6D_o$ (Fig.2 bottom) confirm the stable character of intervals D_o close to δm_N.

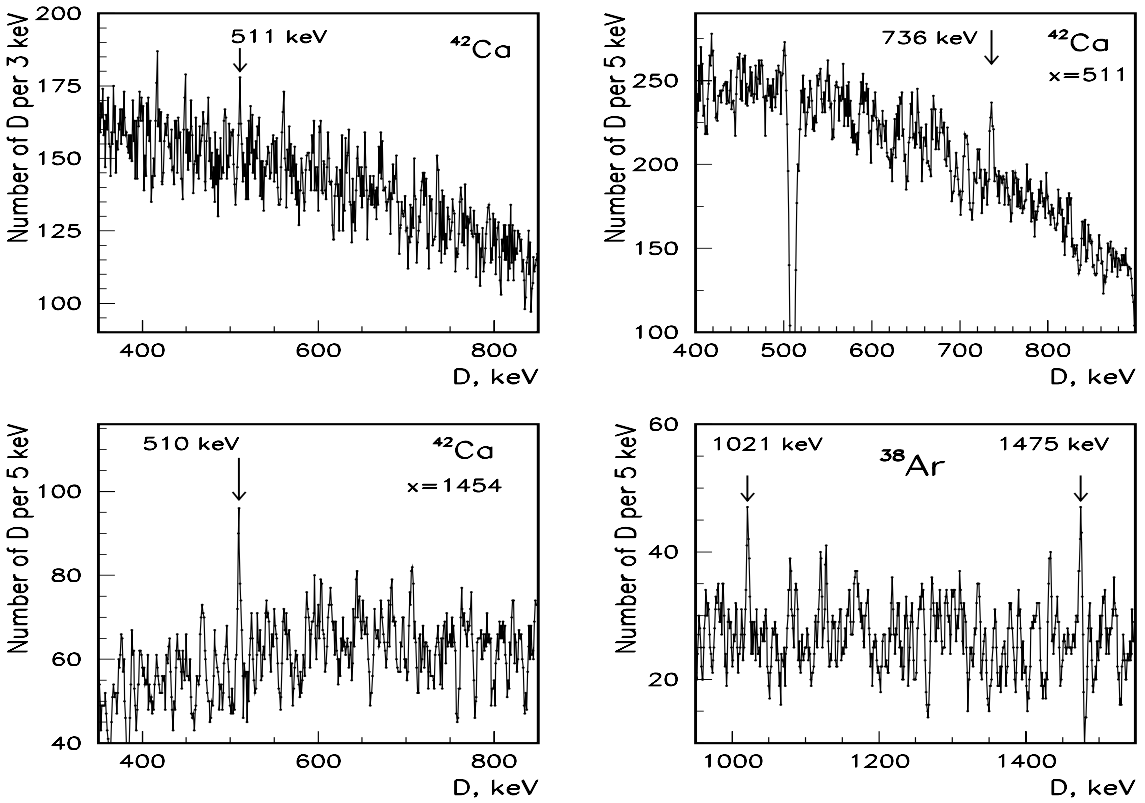

Fig.3. *Top:* Spacing distribution in all excited states of ^{42}Ca (*left*, number of levels n=543 including resonances from $^{41}K(p,\gamma)^{42}Ca$ and $^{38}Ar(\alpha,\gamma)^{42}Ca$ reactions). Results of application of AIM method to the spectrum of ^{42}Ca: D^{AIM}=736 keV for x=511 keV and D^{AIM}=510 keV for x=1454 keV (*top right, bottom left*). Spacing distribution in levels of ^{38}Ar (*bottom right*).

For the check of the discussed stable character of excitations and intervals in light nuclei (related with nucleon mass difference $D_o=\delta m_N$=1293 keV and $\varepsilon_o=2m_e$) data on light nuclei close to ^{40}Ca were used. Clear effect at D=$\varepsilon_o/2$=511 keV in ^{42}Ca (Fig.3 top left, averaging interval Δ=3 keV) was obtained. This interval is a half of D=1021 keV=$\varepsilon_o=2m_e$ in ^{38}Ar (Fig.3 bottom right, ΔE=5 keV) noticed earlier [26-28].

Applying the AIM method to intervals D=x=511 keV in all known states of ^{42}Ca an indication on intervals D^{AIM}=736 keV and 1454 keV=$(9/8)D_o$ were obtained. It is shown in Fig.3 as the distribution of adjacent intervals for x=511 keV (in the upwards direction) and as D^{AIM}-distribution for x=1454 keV (in downwards direction, ΔE=5 keV).

In the discussed group of nuclei around tin three additional effects with D_o were found:

1) The grouping of values E^* $\approx$644 keV$\approx D_o/2$ in Z=47-57 odd nuclei (see Fig.4 top left); four of these values E^* in Sb-isotopes are marked in Table 4 (right).

2) Effect of the monotonic increasing energies of the first excitations in A-odd Sb-isotopes are well-known. Energies in this sequence of levels (in isotopes with ΔN=2, boxed in Table 4) can be expressed as E^*=n$\times$(161 keV=$D_o/8$) starting from the single-particle energy 962 keV=6$\times$161 keV in the near-magic isotope at N=82).

3) Intervals D=322-323 keV=$(2/8)D_o$ and 484-486 keV=$(3/8)D_o$ in neighbor ^{110,111}Cd (N=62,63) were noticed in [27]. Application of AIM-method to x=484-486 keV resulted in D^{AIM}-distributions with maxima at 163-323-647-805-970 keV (all intervals correspond to integer numbers k=1,2,3,4,5 of the period 162 keV=$D_o/8$).

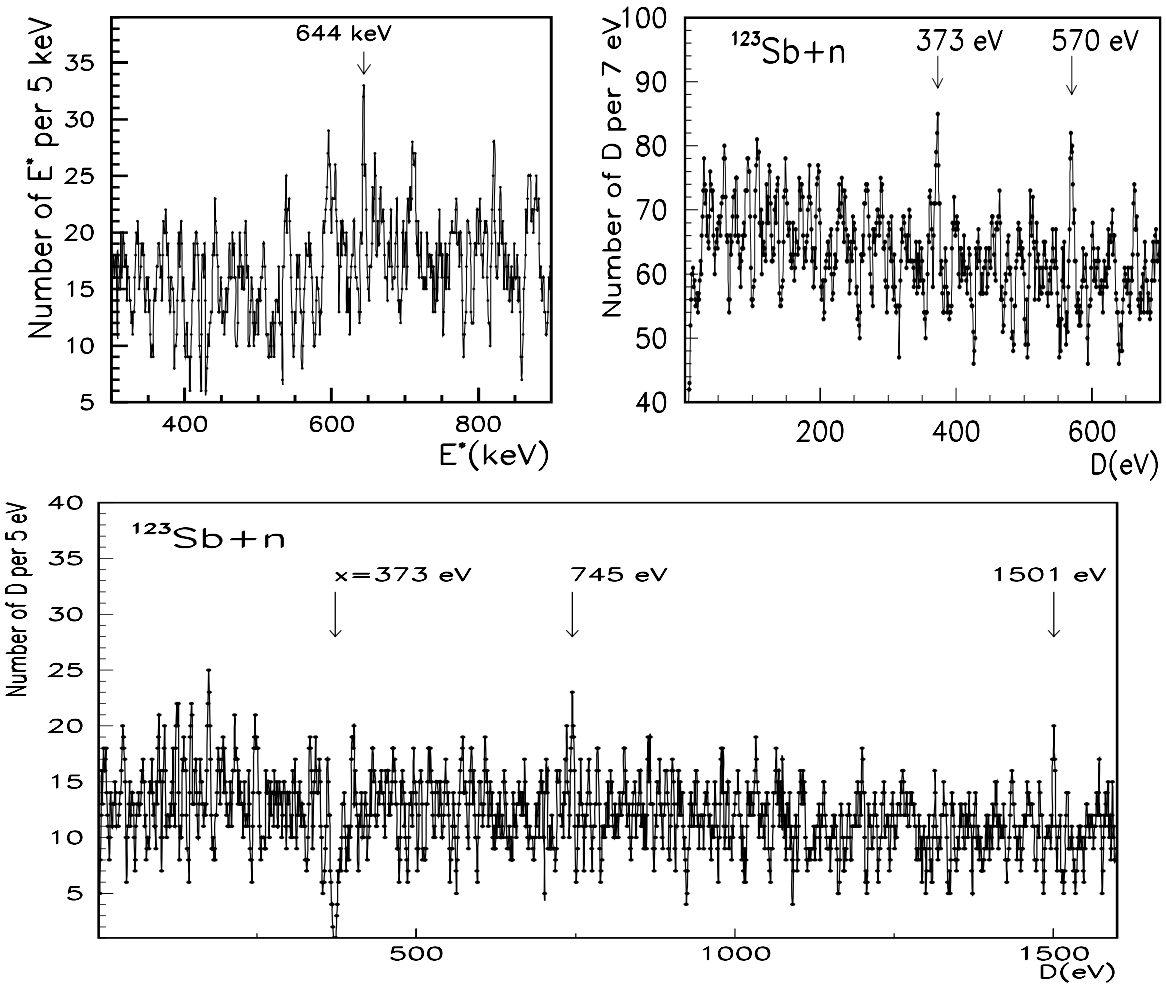

Fig.4. *Top:* Total distribution of excitation energies E^* of nuclei with Z=47-57 [21,19] (*left*); spacing distribution in all neutron resonances of the compound ^{124}Sb [26,1,3] (*right*).
Bottom: Distribution of intervals adjacent to D=x=375 eV in all neutron resonances of ^{124}Sb; maxima at 750 and 1500 eV show the long-range correlation effect in the spectrum [1,3].

Table 4. Comparison of E^* (keV) in Z=51 nuclei with $n\times$(161 keV=$D_o/8$); boxed are E^* of the $5/2^+$ states (g.s. spins are $7/2^*$) with the linear trend and the step of 161 keV starting from the single-particle energy of 962 keV=6×161 keV in ^{133}Sb (N=82) [25].

^AZ	^{133}Sb	^{131}Sb	^{129}Sb	^{127}Sb	^{125}Sb	^{123}Sb	^{125}Sb	^{119}Sb	^{119}Sb	^{113}Sb	^{111}Sb
N	82	80	78	76	74	72	74	68	68	62	60
$2J^\pi$	5^+	5^+	5^+	5^+	5^+	5^+	$3^+,5^+$	1^+	9^+	1^+	(1^+)
E^*	962.0	798.4	645*	491.2	332.1	160.3	644*	644*	970.9	645*	487
n$\frac{D_o}{8}$	969	808	646	484	323	161	646	646	969	646	484
n	6	5	4	3	2	1	4	4	6	4	3

3 New analysis of spacing in near-magic ^{97}Pd, ^{98}Pd

Recently published compilation of excited states of all nuclei [25] allowed new analysis of spacing distribution of many nuclei. Two palladium (Z=46=50-4) isotopes with N=51,52 not considered in the group of Z=48-52 nuclei where selected by the fact that there is a equidistancy in the ground-state excitations (ΔJ=2) in the first of them (with the single valence neutron N=50+1 above the magic core). In both independent spacing distributions stable interval D=D_o=1293 keV is clearly visible (two parts of Fig.5) together with the stable interval D=1060 keV equal to the half of stable E^*=2112-2129 keV in distribution of excitations of nuclei with Z=48-52 in Fig.1. In sum distribution for ^{97,98}Pd the maximum at D=1060 keV has r.m.s. deviation $> 4\sigma$ (Fig.6) and additional maxima at D=648 keV$\approx D_o/2$ and D=512 keV=$\varepsilon_o/2$ are clearly seen.

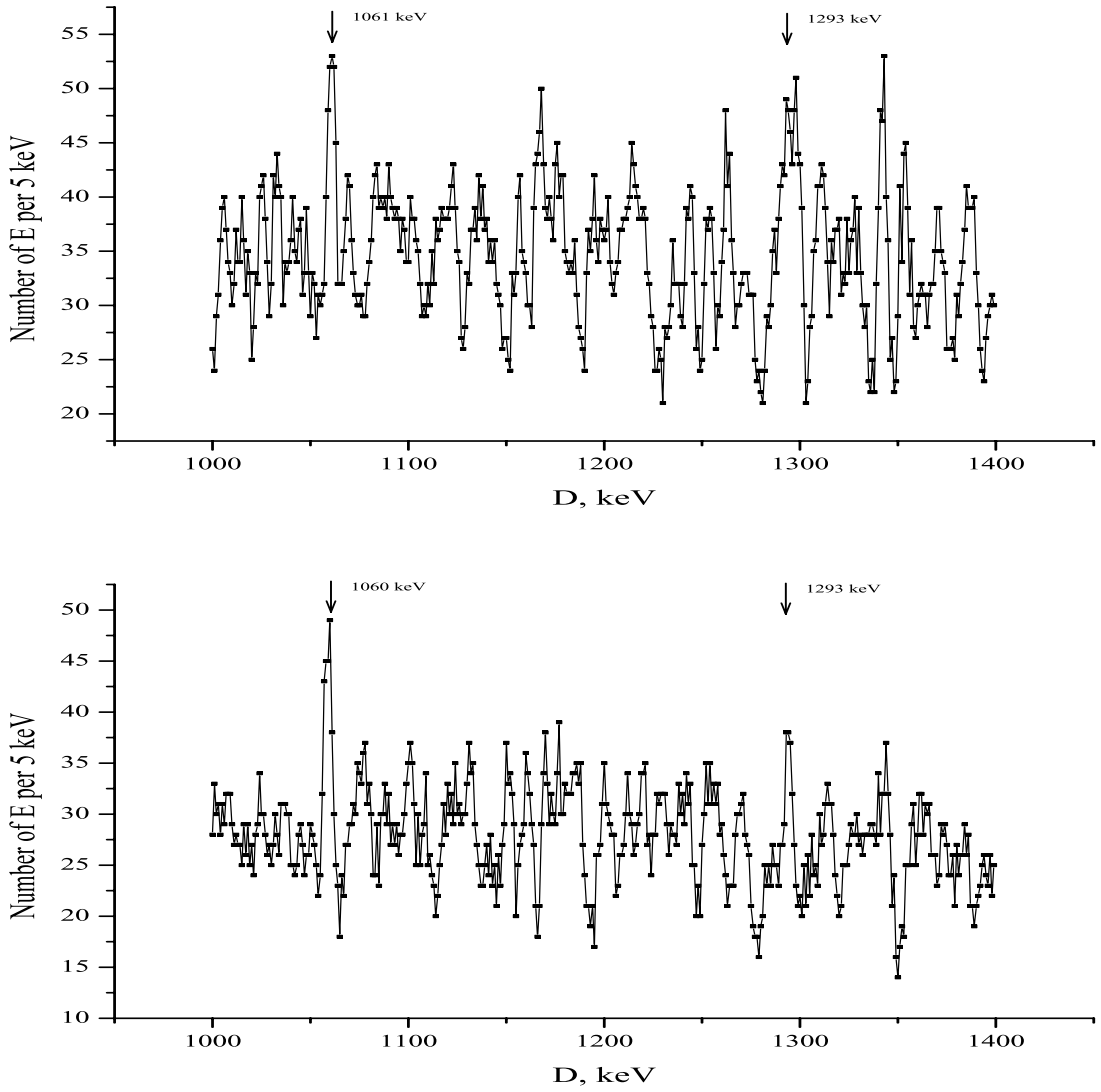

Fig.5. Spacing distribution in ^{97}Pd (*top*) and the same in ^{98}Pd (*bottom*). Arrows mark positions of stable intervals in both energy spectra, the second grouping in ^{97}Pd includes equidistant ΔJ=2 excitation in this nucleus with one valence neutron (N=51).

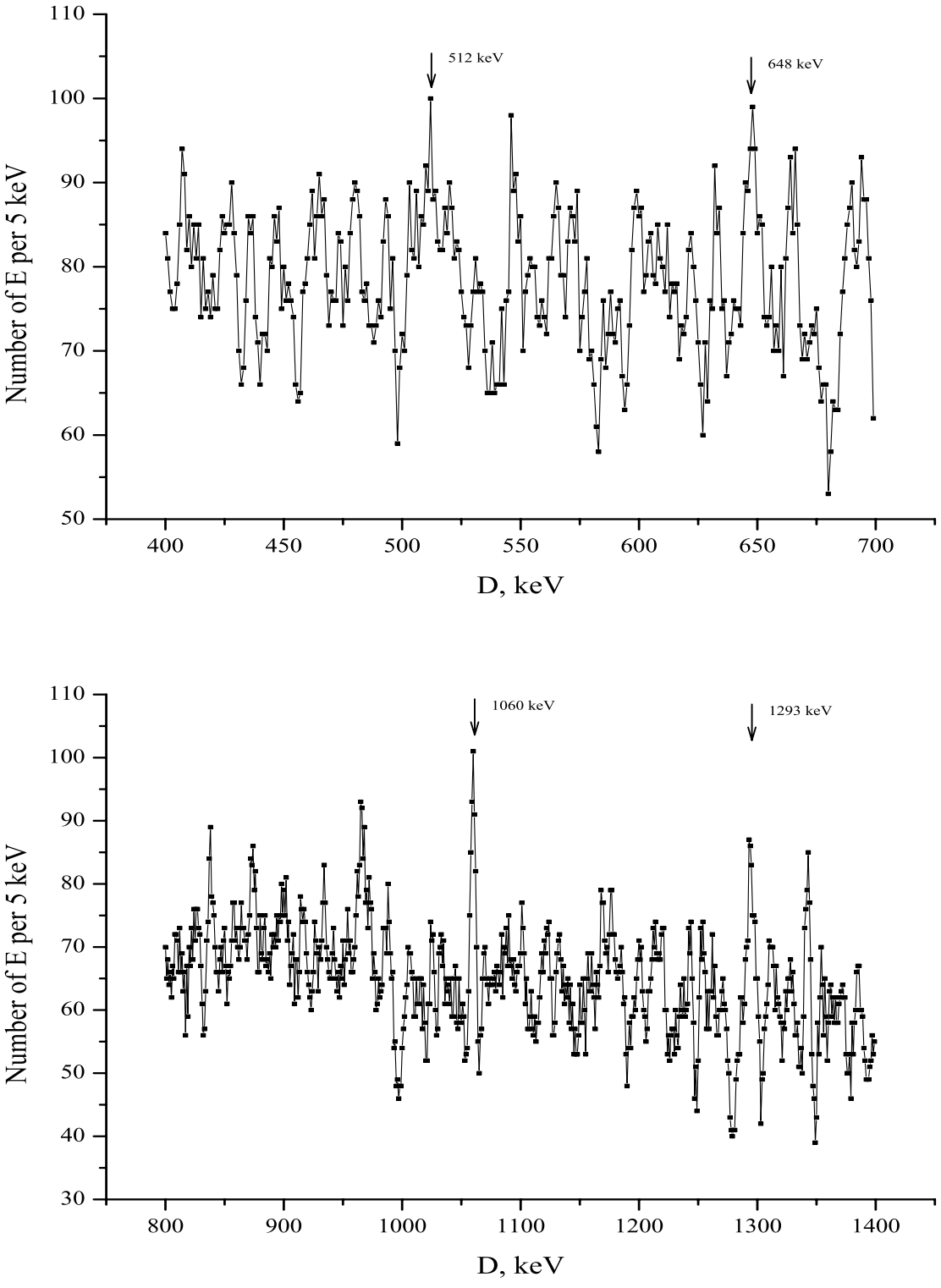

Fig.6. Sum of spacing distributions in ^{97,98}Pd in two different energy regions, intervals 648 and 1293 keV are in approximate 1:2 relation, all intervals are marked by two asterisks in Table 2.

4 Inclusion of neutron resonance data

In neutron resonances of near-magic compound ^{124}Sb a system of stable superfine-structure intervals multiple with 5.5 eV=$\delta''/2$ [15] was found as series of intervals with periods 55 eV=$5\delta''$ and 88 eV=$8\delta''$ [26,3]. In spacing distribution stable intervals D=373 eV=$17\times2\delta''$ and 570 eV=$13\times4\delta''$ are clearly seen (Fig.4 top right). Intervals D^{AIM}=745 eV=$17\times4\delta''$ and 1501 eV=$17\times8\delta''$ (two- and fourfold-values of initial x) were found by AIM-method.

The interval D=749 eV=$17\times4\delta''$ was found also in ^{80}Br (Fig.7 bottom right). Intervals D=748 eV and D=1495–1497 eV=$17\times8\delta''$ were found in neighbor ^{104}Rh and ^{105}Pd (Fig.7). By the AIM method (x=1497 eV, ^{106}Pd) intervals D^{AIM}=7498 eV$\approx5\times$1497 (Fig.7, top right, averaging interval 5 eV) are shown. A simultaneous appearance of intervals D_o, $2D_o$ and $D_o/2$ in low-lying levels of ^{odd}Sb, ^{97,98}Pd and small intervals multiple with 750 eV in resonances of ^{124}Sb, ^{104}Rh, ^{106}Pd were used for the indirect check of intervals D_o. If compare small interval/period 1499.6(4) eV=7498 eV/5 and large interval D=1293(2) keV=D_o in ^{97,98}Pd (as δm_N=1293.3 keV) despite a difference of 8 neutrons between ^{98}Pd (low energy) and ^{106}Pd (high excitations) their ratio 1.4996 keV/1293.3 keV=1.1595(3)$\cdot10^{-3}$ coinciding with $\alpha/2\pi$ will be found (see also [21,27,29,30]).

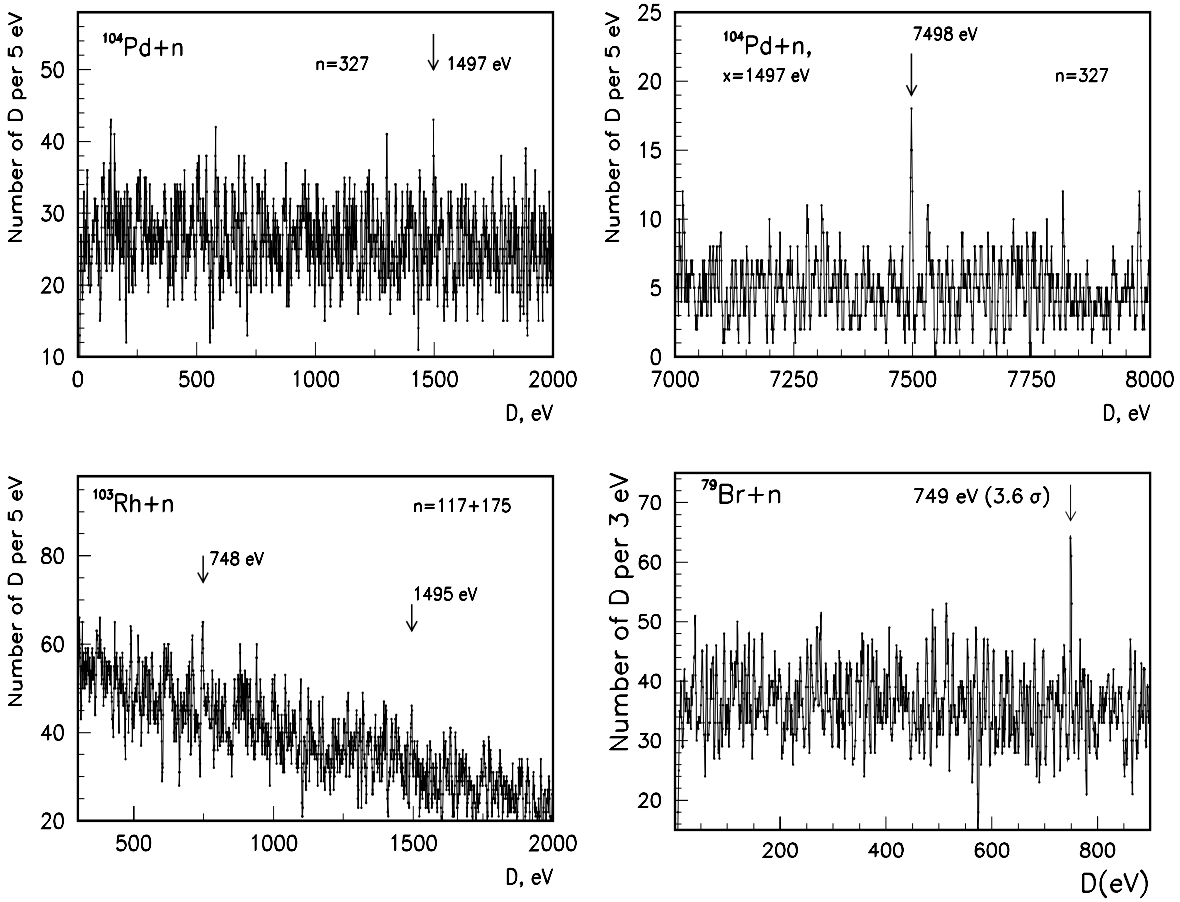

Fig.7. *Top:* Spacing distribution in neutron resonances in compound nucleus ^{105}Pd (number of resonances n=327) (*left*) and distribution of intervals adjacent to x=1497(2) eV (distribution in downwards direction); interval D^{AIM}=7495(2) eV is close to 1497 eV$\times$7485(10) eV (*right*). *Bottom:* Spacing distributions in neutron resonances of compound nucleus ^{104}Rh (sum of distributions for 117 s-resonances and 175 p-resonances); the same for all resonances in ^{76}Br.

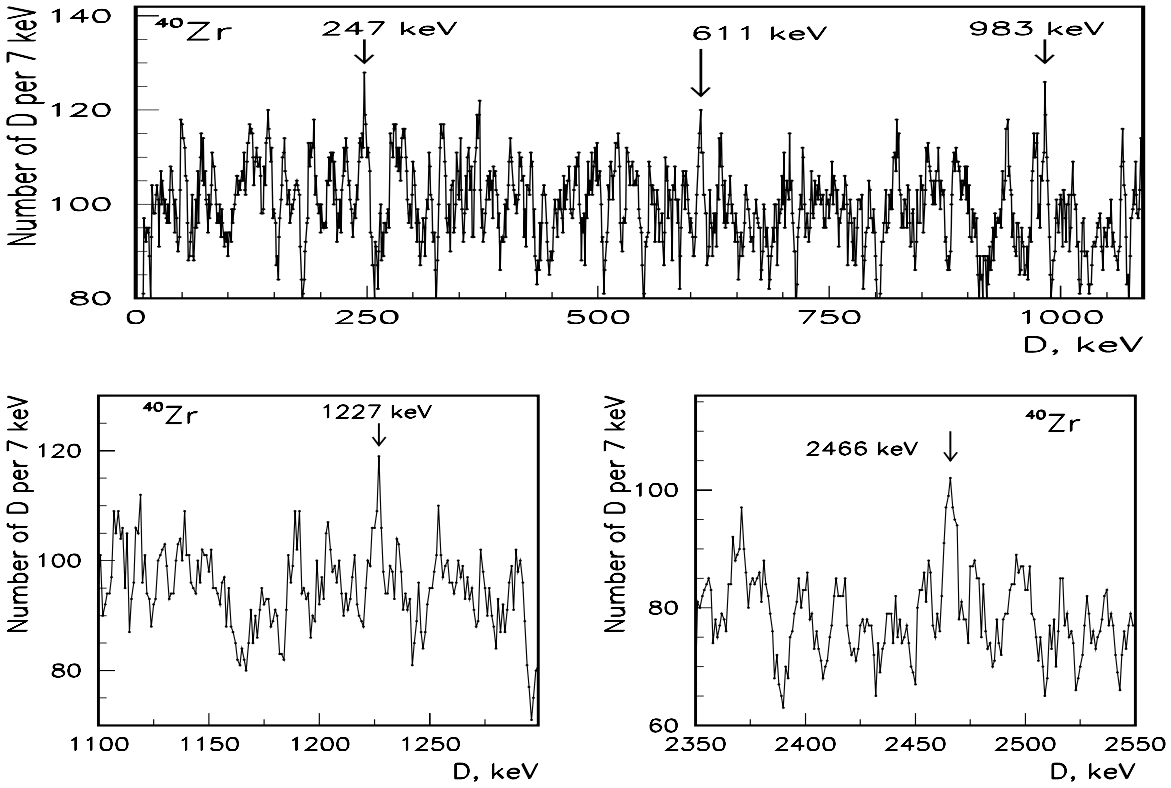

Fig.8. Spacing distribution in levels of ^{90}Zr (number of states n=355)); marked period 247 keV.

Another application of neutron resonance data is the expanding of spectroscopic information for near-magic nuclei. For example, results from the performed earlier analysis [28] of neutron resonance data for target nucleus ^{89}Y can be considered as the supplementary to the information obtained from analysis of data on low-lying excitation of nuclei around Zr [31-34] from new high-resolution γ-scattering experiments (not included in [25]).

In Fig.8-11 results of the study of grouping effects in spacing distribution of levels in ^{88}Sr, ^{89}Y, ^{90}Zr, ^{92,98,100}Mo and ^{141}Pr (mainly (γ,γ) data) are presented. Clearly seen periodicity in maxima in spacing distribution of the double-magic nucleus ^{90}Zr (period of 247 keV is marked in Fig.8 with arrows). Intervals 611 keV-1227 keV-2466 keV form an exact ratio 1-2-4 with D=611 keV=(5/2)247 keV. Intervals D=247 keV and D=245 keV in two independent spacing distributions for ^{98}Mo and ^{100}Mo (see top and bottom parts of Fig.9) can be related as 2-3-5 to intervals 369 keV and 611 keV in spacing distribution and D^{AIM}-distribution in these nuclei (for x=53 keV, marked with arrow). Small interval D-53 keV in ^{98}Mo coincides with splitting 734.8 keV-787.4 keV in low-lying 0^+ and 2^+ excitations of this nucleus, while the 0^+ excitation is close to 3×247 keV=741 keV.

Spacing distributions in ^{89}Y and ^{90}Y and D-distribution in highly-excited states of ^{90}Y seen as neutron resonances are shown in Fig.10. Study of neutron resonance data with AIM-method allowed conclusion that intervals 480 keV and 510 keV seen in low-energy part of spectra preserve their discrete character at higher excitations. As a result intervals D=478.6 keV and 511.0 keV (with spacing 32.5 keV) are appearing simultaneously [28]. The maximum at D^{AIM}=511.0 keV is shown here (Fig.10 bottom left) for x=478.5 keV (in downwards direction). Intervals 480 keV in ^{90}Y, 322 keV in ^{88}Sr and D=1292 keV in the near-magic ^{141}Pr (Fig.10 bottom right) are close to intervals in other nuclei (Table 2).

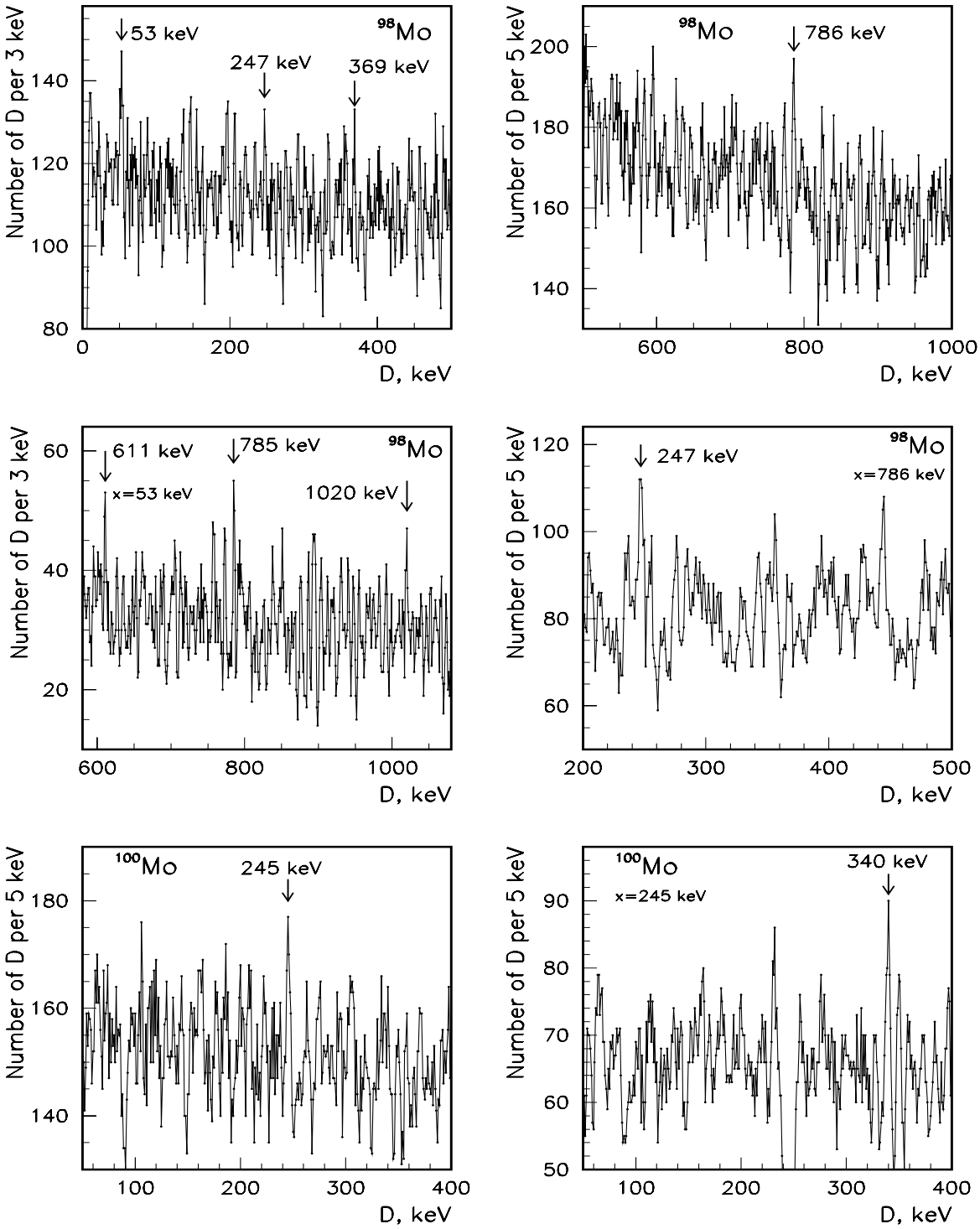

Fig.9. *Top:* Spacing distribution in levels of ^{98}Mo (number of states n=492, ΔE=3 and 5 keV). *Center:* Distribution of intervals adjacent to D=x=53 keV and 786 keV in spacing of ^{98}Mo. *Bottom:* Spacing distribution in ^{100}Mo (number of states n=440) and D^{AIM}-distribution for x=245 keV (in upwards direction) for this nucleus.

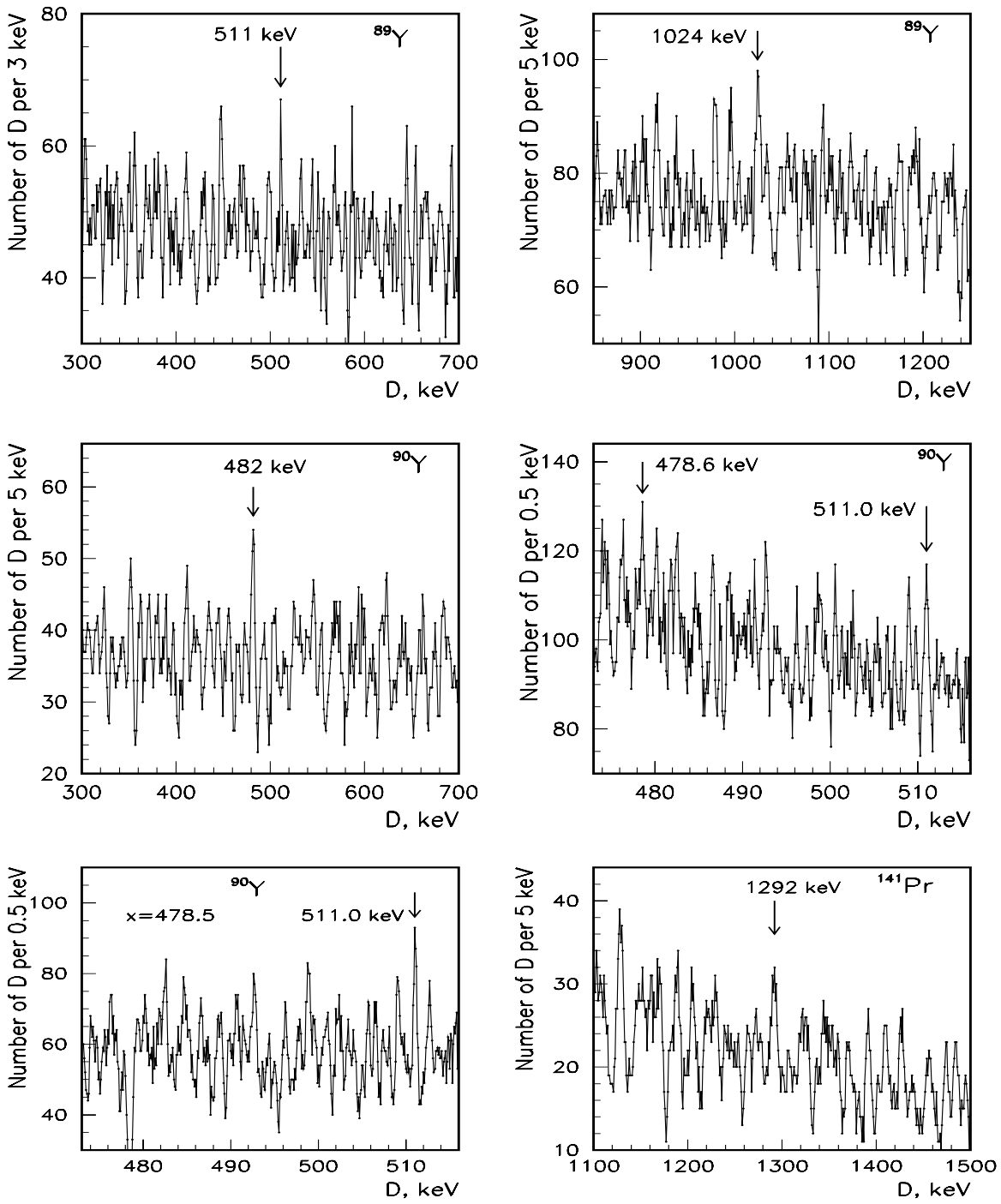

Fig.10. *Top:* Spacing distribution of levels in ^{89}Y (number of states n=388, ΔE=3 and 5 keV). *Center:* Spacing distribution of levels in ^{90}Y (n=190) in low-energy region [25], ΔE=5 keV (*left*) and spacing distribution of neutron resonances of ^{90}Y (n=692 [3], ΔE=0.5 keV). *Bottom:* Distribution of intervals adjacent to D=x=478.5 keV in resonances of ^{90}Y; maximum at D^{AIM}=511.0 keV (in downwards direction) means that intervals 480 keV–510 keV are frequently appearing together (*left*); Spacing distribution of levels in ^{141}Pr (n=166 (*right*); interval D=1292 keV=D_o in the near-magic ^{141}Pr (Fig.11 bottom right) and intervals 480 keV in ^{90}Y and 322 keV in ^{88}Sr (Fig.11) as well as D=648 keV and 1293 keV in ^{97,98}Pd (Fig.5,6) are close to the systems of above discussed intervals in light nuclei (Fig.2) and in nuclei around tin (Fig.4).

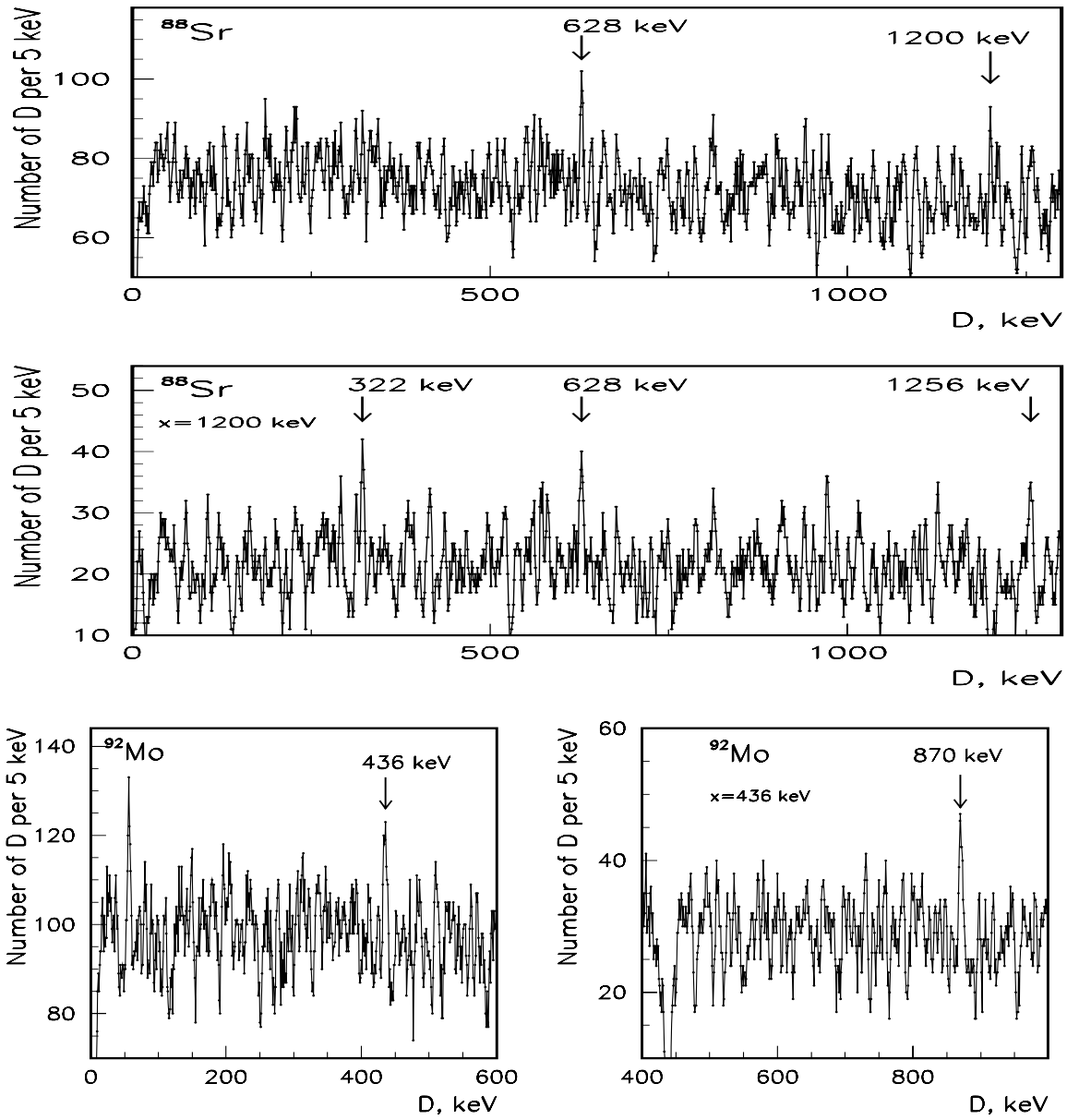

Fig.11. *Top:* Spacing distribution of levels in ^{88}Sr (number of states n=254).
Center: Distribution in adjacent intervals (for x=1200 keV) in levels of ^{88}Sr.
Bottom: D-distribution in ^{92}Mo (number of states n=434); D^{AIM}-distribution for x=436 keV.

Maxima in spacing distributions in ^{88}Sr and ^{92}Mo shown in Fig.11 correspond to stable intervals 628 keV and 436 keV frequently forming a sequence of intervals (see D^{AIM}-distributions for x=1200 keV and x=436 keV). More data on spin values are needed for the development of microscopic models of the above discussed systematic effects.

Intervals 340 keV – 1020 keV in ^{100}Mo (marked in AIM-distributions, Fig.9) and intervals D=511 keV, 1024 keV marked in spacing distribution in the near-magic ^{89}Y (Fig.10 top) are forming 2-3-6 relation. We observe the same relation 13-18 in values of adjacent intervals D=245-340 keV in ^{100}Mo (nucleus with two valence protons), in values of intervals D=511-736 keV in ^{42}Ca (two valence neutrons, Fig.3 top) and intervals D=1021-1475 keV in ^{38}Ar (two holes in ^{40}Ca, Fig3. bottom). Hence all these independent intervals are included in the corresponding lines m=2,3,6 of Table 2 (n=13 and 18).

5 Conclusions

Nuclear data files after inclusion of recent high-resolution results and resonance data provide an information for further development of microscopic nuclear models for quantitative description of the observed tuning effects in nuclear excitation. Simultaneously they provide a direct confirmation of noticed long-range correlations in nuclear binding energies which in its turn can be considered as an indirect support of the reality of long-range correlations in tuning effects in particle masses including the observed and discussed elsewhere [35] the distinguished role of particle mass splitting: m_e, δm_N, δm_π, m_μ, m_π.

References

1. S.Sukhoruchkin, *Proc. ISINN-13*, JINR E3-2006-7, p.83; Z.Soroko et al., *ibid*, p.205
2. Z.Soroko et al., *Proc. ISINN-16*, Dubna, 2008, JINR E3-2009, p.139 (2009).
3. F.Gunsing et al. *Springer LB.* Ed.H.Schopper v. I/24 (2009), see also v. I/16BC
4. S.I.Sukhoruchkin, *Proc. Symp. Discrete'08* Valen., 2008, Jour. Phys. IOP (2009).
5. S.I.Sukhoruchkin, *Int. Rev. Phys. 2,* 239 (ISSN 1971-680X, 2008).
6. S.I.Sukhoruchkin, *Izv. RAN, ser. Fiz.*, v. 73. no. 6, p.873 (2009).
7. S.I.Sukhoruchkin, *Proc.13th. Symp.Capt.Gamma-Rays,* Koeln, AIP 1090, 641 (2008).
8. S.I.Sukhoruchkin, *Proc.17th. Int. Spin Physics Symp.,* Kyoto, AIP 915, 272 (2007).
9. S.I.Sukhoruchkin, *Proc. Conf. Nucl. Data Sci. Tech.,* Nice, CEA EDP) 179 (2007).
10. S.I.Sukhoruchkin, *Proc. 6th Conf. Persp. Hadr. Phys.,* Trieste, AIP 1056, 55 (2008).
11. S.I.Sukhoruchkin, *Proc. 2nd Int. Conf. Neutr. Cross Sec.,* Wash., vol,2, 923 (1968).
12. S.I.Sukhoruchkin, *Stat. Prop. Nuclei,* Ed. J.Garg, Plenum Press N.-Y, p.215 (1972).
13. Z.N.Soroko, S.I.Sukhoruchkin, D.S.Sukhoruchkin, *Nucl. Phys.* A 680 p.254c (2001).
14. S.I.Sukhoruchkin, *IAEA Nucl. Data. for Reactors*, Paris, v.1, p.159 (1966).
15. K.Ideno and M.Ohkubo *Jour. Phys. Soc. Japan*, 30, 621 (1971).
16. S.I.Sukhoruchkin, *Proc. ISINN-6*, JINR E3-98-202, p.343; *ibid* pp.332 and 141.
17. S.I.Sukhoruchkin, Tuning Effect in Nucl. Data *Proc. ISINN-8*, E3-200-192, 428,420.
18. S.I.Sukhoruchkin, *Proc. 10th Conf. Intersect. Part. Nucl. Phys.* (2009) to be publ.
19. Z.Soroko et al., *Proc. ISINN-10*, JINR E3-2003-10, pp.289, 299, 308.
20, S.I.Sukhoruchkin, *Nucl. Phys.* A (2007)
21. S.I.Sukhoruchkin et al.*Proc.11th.Symp.Capt.Gamma-Rays*,Prag, WS, 825,829 (2003)
22. O.I.Sumbajev, A.I.Smirnov, L.N.Kondurova, *JETF* 61, 1276 (1971)
23. E.E.Witmer, Phys. Rev. 95 (1954) pp.610, 667.
24. ENDSF, *Nuclear Data Sheets*, current issues, Academic Press.
25. S.Sukhoruchkin, Z.Soroko *Springer LB.* Ed.H.Schopper v. I/19ABC, I/22AB (2009).
26. S.I.Sukhoruchkin et al.*Proc.10th.Symp.Capt.Gamma-Rays*,Santa Fe, AIP-529, 703
27. S.I.Sukhoruchkin, *Proc. ISINN-9*, JINR E3-2001-192, p.351; *ibid* p.342 (2001).
28. Z.N.Soroko et al., *Proc. ISINN-7*, JINR E3-99-212, 1999, p.313 (1999).
29. S.Sukhoruchkin, *Proc. ISINN-2*, JINR E3-94-419, p.234, 326 (1994).
30. S.Sukhoruchkin, *Proc. ISINN-3*, JINR E3-95-3077, p.182, 230 (1995).
31. R.Schwengner et al. Phys.Rev.C 76, 034321 (2007).
32. N.Benouaret et al. Phys.Rev.C 79, 014303 (2009).
33. R.Schwengner et al. Phys.Rev.C 78, 064314 (2008).
34. G.Rusev et al. Phys.Rev.C 73, 044308 (2006); G.Rusev, Dissertation, Dresden (2006).
35. S.I.Sukhoruchkin, The origin of tuning effects in nuclear data, these proceedings.